Newton's rings in near-field optics

Lori S. Goldner,[a] Jeeseong Hwang, Garnett W. Bryant, and Michael J. Fasolka
National Institute of Standards and Technology, Gaithersburg, Maryland 20899

P. P. Absil, J. V. Hryniewicz, F. G. Johnson, H. Shen,[b] and P.-T. Ho
Laboratory for Physical Sciences and Department of Electrical and Computer Engineering, University of Maryland, College Park, Maryland 20742

(Received 28 June 2000; accepted for publication 5 December 2000)

We show how Newton's rings manifest themselves in near-field scanning optical microscopy and discuss how this effect can be used with topographic imaging to measure correlated roughness of thin films. In conventional optics, transmission through a thin nonabsorbing film depends on film thickness when multiple reflections from the film boundaries are coherent. Measurements and modeling of the transmission through thin films illuminated by a near-field probe show that these oscillations are present despite the large distribution of transverse wave vectors needed to describe light from the probe. © *2001 American Institute of Physics.* [DOI: 10.1063/1.1343850]

In transmission near-field scanning optical microscopy (NSOM), light from the near-field of a subwavelength aperture is used to illuminate a sample and collected with far-field optics (i.e., a microscope objective) on the opposite side of the sample.[1,2] An image is formed by scanning the sample. While super-resolution can result from imaging in this fashion, a variety of artifacts resulting from topographic and far-field interactions may obscure the true optical resolution of the image.[3,4] Here, we discuss how variations in local film thickness can be measured using variations in the transmission through the film, an effect analogous to Newton's rings, or fringes of equal film thickness,[5] in far-field optics. This effect, due to multiple reflections from the film boundaries, involves only the propagating and not evanescent components of the near-field illumination. This means that the lateral resolution for measured changes in film thickness will be similar to the far-field case, about one wavelength. Nonetheless, the combination of optical and topographic imaging provided by NSOM will permit us to directly measure the local correlated roughness of thin films on patterned substrates. For many samples, it is important to note that near-field imaging of surface features will be obscured by this film thickness sensitivity of transmission NSOM. Modeling of this effect is, therefore, important for correct interpretation of NSOM images, as well as for measuring correlated roughness.

To demonstrate this effect, we use low molecular weight[6] (3.7 K) polystyrene (PS) prepared by spin coating (PS 2% weight in toluene) at 209 rad/s (2000 rpm) on a clean No. 1 glass coverslip. Annealing (120 °C for 24 h) induces dewetting characterized by the formation of droplets. Figure 1 shows simultaneous optical and topographic data taken at an edge of a PS droplet. The NSOM probe used is a pulled optical fiber coated with approximately 150 nm of Al (typical aperture sizes were $\leqslant 150$ nm). Light at 488 nm from the probe is collected with an 0.75 numerical aperture (NA) objective on the opposite side of the sample and detected with the use of a Si photodiode. Contours that represent the simultaneously acquired topographic data are superimposed on the transmission image. Topographic data are collected using electro-mechanical detection of the tip dither amplitude (shear-force detection in constant gap mode).[7] The glass surface is clearly visible as the flat region on the left-hand side. The overall transmission is dependent on the local scattering properties (i.e., the roughness) of the glass (or PS) surface, and is difficult to calculate; we make no attempt to do so here. On the right-hand side of Fig. 1, as the PS thickens away from its edge, interference fringes are clearly visible. A line cut through the image showing both topographic and optical data is shown at the bottom of Fig. 1.

We use a three-layer model to understand the thickness dependence of transmission NSOM. The first layer is a semi-infinite air layer between the tip and sample. The second layer is a uniform PS film of thickness z_{film}, nominal index of refraction $n_{\text{film}}=1.59$. The third layer is a semi-infinite substrate layer (glass, $n_{\text{glass}}=1.4$). The tip is placed a distance z_{tip} from the film surface. In our model, the tip provides a fixed source field incident on the film. We model this field using the Bethe–Bouwkamp solutions for the near-field of an aperture in a perfectly conducting thin film.[8–10] The transmission of the source field through the film and into the substrate is found using the appropriate field matching at each interface.[10] All light that propagates to the far field in the substrate inside the solid angle defined by the collection optic NA is included to determine the transmitted light intensity. By choosing a substrate with index $n_{\text{sub}}>1$, we can model collection with NA>1.

In Fig. 2 we show the trends in our data and the trends in the calculated transmission through a PS film illuminated by a 100 nm diameter aperture for different collection optic NAs. Here, the maximum transmission of both the data and calculations have been normalized to 1. The data, which are offset from the theory for clarity, are proportional to the transmission intensity at a given thickness averaged over an entire image. The spacing between the fringes is, as in conventional optics, determined primarily by the wavelength of light and is approximately $\lambda/2n_{\text{film}}$. This spacing is modu-

[a]Electronic mail: lori.goldner@nist.gov
[b]Also at: U. S. Army Research Laboratory, Adelphi, Maryland 20783.

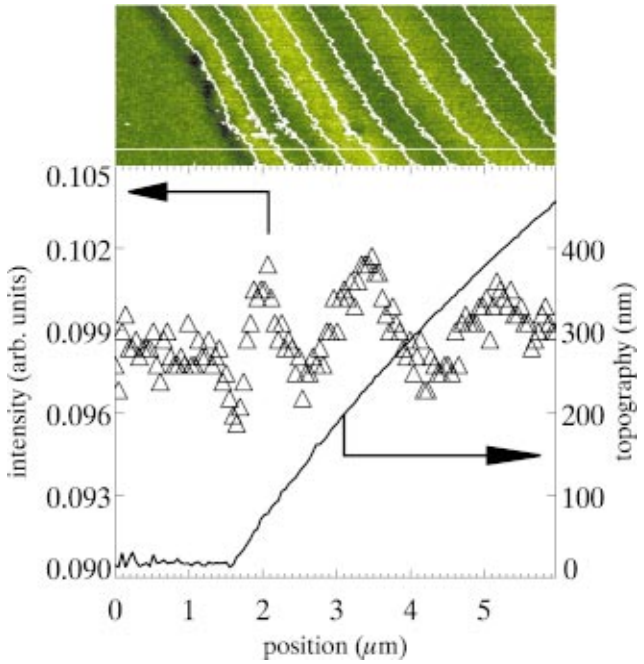

FIG. 1. (Color) NSOM transmission image taken at the edge of a dewetted polystyrene droplet. Contours of constant topography are superimposed in white, 46 nm apart in height. Topographic and near-field data from the horizontal line shown in white are plotted below the image.

lated by a tip and NA dependent *envelope* that depends on the lateral k-space distribution of light emitted by and collected from the tip. The first minimum in the *envelope* occurs for the thickness at which the central and marginal rays of the optical system have a phase difference along the optical axis of π through the film. The amplitude of the fringes *and* envelope depend upon the details of the tip field. For low NA collection optics the first envelope minimum occurs for thicker films since forward scattered k vectors are involved primarily. For larger NA, the first minimum occurs for successively thinner films and the modulation is deeper. These

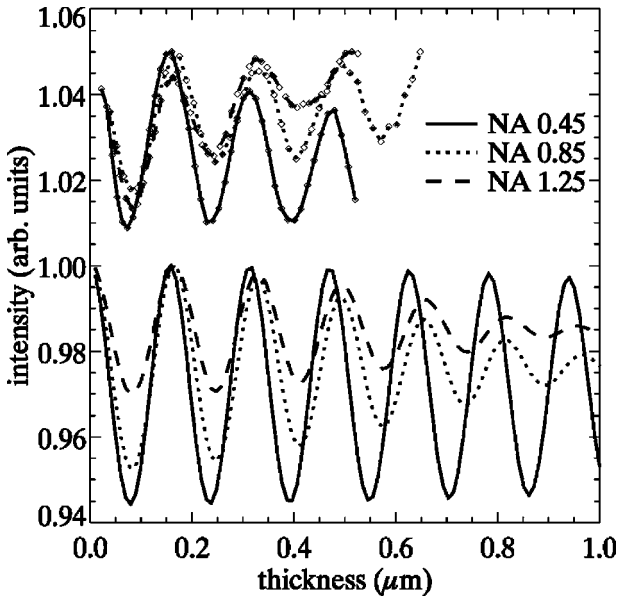

FIG. 2. Theoretical and measured transmission intensity vs PS film thickness for 3 different NA collection optics. All data sets have been normalized to a maximum value of 1; the experimental values are offset 0.05 on this scale.

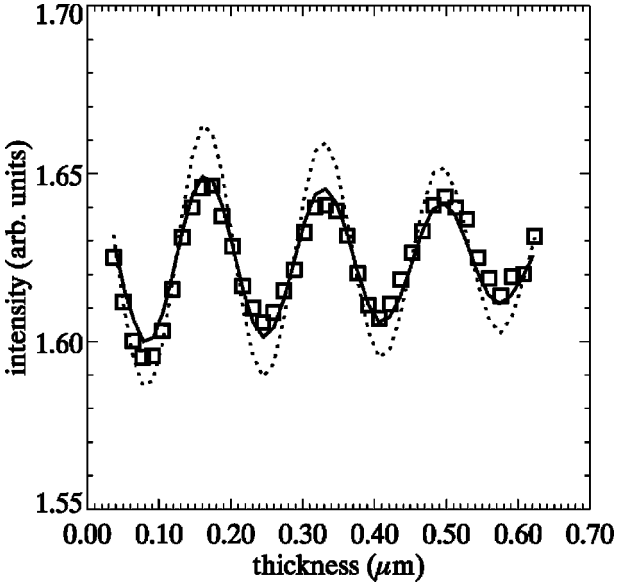

FIG. 3. Intensity vs PS film thickness. Squares: experimental results. Dotted line: fit of model to data without lateral averaging. Solid line: fit of model to data with lateral averaging.

trends can be seen in both the data and the model. Even with the large distribution of momentum vectors present for these subwavelength sources, fringes are evident in the data with a contrast, $(I_{\max}/I_{\min}-1)$ where I is the transmitted intensity, of approximately 4%.

A few discrepancies between theory and data merit discussion. In the absence of surface scattering, the thinnest regions of the film would have the highest transmission. Instead, we see a shift from glass to PS that is dependent on local scattering, i.e., the details of the glass and PS surface. In addition, our model does not account for the sloping surface of the PS and the accompanying polarization dependence of the transmission, which also shifts the overall level of scattering between the glass and PS. Neither of these effects should shift the position of the interference peaks al-

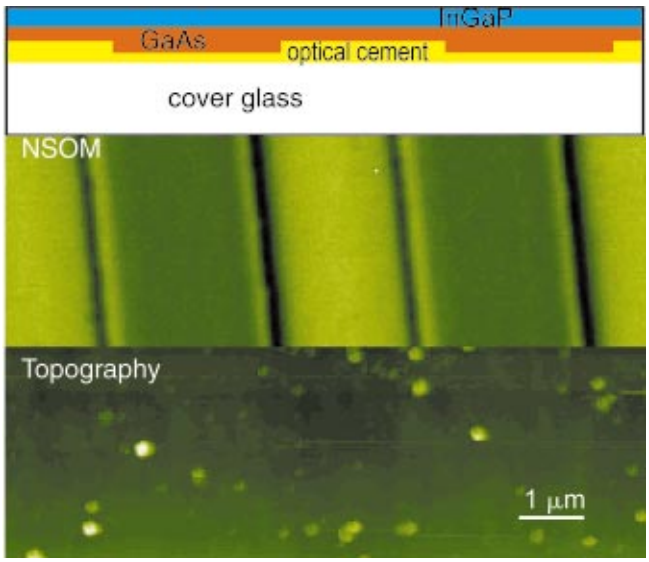

FIG. 4. (Color) Top: diagram of sample (side view). InGaP is 50 nm thick; GaAs layer is 100 nm with 56 nm deep lines etched into it. Center: near-field transmission image, 9.83 μm by 3.20 μm. Bottom: corresponding topographic image.

though the fringe contrast may be affected. The calculated contrast is typically 50% greater than the experimental contrast. In addition to the effects mentioned, this could be due to the variation of PS thickness under the tip, also not accounted for in this model. Since the interference rings depend on multiple reflections from the PS surface, the transmitted signal probes a lateral region of order λ in diameter under the tip. Finally, the details of the tip field also affect the contrast, with smaller aperture tips generally resulting in smaller contrast.

As an example we show in Fig. 3 two fits to data from an image taken at NA=0.85. The only adjustable parameters are the piezo tube calibration factors (three parameters, up to second order in the voltage) and a scale factor to account for overall throughput. The dotted line is a fit of the model and clearly shows the discrepancy between modeled and actual fringe contrast. The solid line is a fit that attempts to take into account the slope of the PS surface by averaging the calculated transmission at five points along the thickness gradient. These points have thicknesses corresponding to $l_i \times |\nabla t|_{t_0} + t_0$ where $|\nabla t|_{t_0}$ is the absolute value of the gradient at a given thickness t_0 and $l_i = (-488, -244, 0, 244, \text{and } 488\ \text{nm})$ are the five lateral positions. Averaging over 2λ clearly can account for the decrease in contrast, although it is unlikely that this is the entire cause of the discrepancy. This does, however, put an upper limit of 2λ on the lateral resolution of this technique for measuring film thickness. The two fits, while clearly different, result in piezo tube calibrations that are indistinguishable to within the uncertainty in the fits. For Fig. 3, the linear term was $10.1\,\text{nm/V} \pm 0.1\,\text{nm/V}$ (standard deviation) and the second order term was $0.018\,\text{nm/V}^2 \pm 0.002\,\text{nm/V}^2$. Calibrations performed in this fashion have an advantage over the use of a reference artifact, which requires separate scans of the artifact and cannot account easily for changes in offset voltage or piezo aging.

In Fig. 4, we show an example of typical data on a semiconductor sample with topography uncorrelated from its buried structure. The sample consists of 50 nm of InGaP, followed by 100 nm of GaAs. A test pattern is etched into the GaAs. The sample is mounted with the patterned side down on a transparent substrate (glass coverslip) using optical cement. The strong absorption and high index at 488 nm (the field decay length is $\approx 150\,\text{nm}$ and the real part of the index of refraction is ≈ 4.4) results in deep interference fringes that are strongly modulated by an exponential decay with film thickness. The difference in transmission between etched and unetched regions is a combination of these two effects. Interference fringes due to a rapidly changing thickness are clearly visible at the edges of the pattern. Lateral interferences may also be present in systems where the features are closer together or the absorption length is longer. The asymmetry of the features in this example is not yet understood but may be due, for example, to tip aperture or sample asymmetries. The topography, which is mostly flat with small surface contaminant particles (typical height about 50 nm), is obviously uncorrelated with the modulation in film thickness. A complete model for this system would include the InGaP layer and be able to account for the lateral structure of the system.

We propose that this phenomenon may provide a quantitative method for measuring the local correlated roughness of thin films on patterned substrates. A complete understanding of substrate roughness propagation in polymeric systems, for example, is crucial to the design and development of three-dimensional device architectures. Here, we have shown how transmission data obtained in transmission NSOM can be modeled and used to determine the local thickness of a film, while topographic information is independently acquired through shear-force surface tracking commonly used in NSOM. We expect that future enhancements to the theory will enable us to account properly for surface and substrate curvature and slope, as well as lateral interferences that have been discussed elsewhere[4] and may be important in films with sharp, closely spaced features.

The authors would like to thank the NIST Advanced Technology Program's organic electronics focussed program for helping to fund this project. The work at the University of Maryland was funded in part by NIST Contract No. MD980403-7499.

[1] D. W. Pohl and L. Novotny, J. Vac. Sci. Technol. B **12**, 1441 (1994).
[2] E. Betzig and J. K Trautman, Science **257**, 189 (1992).
[3] B. Hecht, H. Bielefeldt, Y. Innoye, and D. W. Pohl, J. Appl. Phys. **81**, 2492 (1997).
[4] A. J. Campillo, J. W. P. Hsu, and G. W. Bryant (unpublished).
[5] M. Born and E. Wolf, *Principles of Optics*, 4th ed. (Pergamon, Oxford, 1970), pp. 286–291.
[6] According to International Standards Organization (ISO) 31-8, the term ''molecular weight'' has been replaced with the ''relative molecular mass,'' symbol *Mr*. The conventional notation, rather than the ISO notation, has been employed for this publication.
[7] P. Derose, J. Hwang, and L. S. Goldner, Proc. SPIE **3272**, 93 (1998).
[8] H. A. Bethe, Phys. Rev. **66**, 163 (1944).
[9] C. J. Bouwkamp, Philips Res. Rep. **5**, 321 (1950); C. J. Bouwkamp, *ibid.* **5**, 401 (1950).
[10] G. W. Bryant, E. L. Shirley, L. S. Goldner, E. B. McDaniel, J. W. P. Hsu, and R. J. Tonucci, Phys. Rev. B **58**, 2131 (1998).